Report

Current Biology

The Compact Body Plan of Tardigrades Evolved by the Loss of a Large Body Region

Highlights

- Several Hox genes were lost early in the tardigrade lineage (phylum Tardigrada)
- The tardigrade *Hypsibius dujardini* does not possess an organized Hox cluster
- Tardigrade segments are primarily homologous to head segments in arthropods
- Tardigrades have lost an intermediate region of the body axis

Authors

Frank W. Smith, Thomas C. Boothby, Ilaria Giovannini, Lorena Rebecchi, Elizabeth L. Jockusch, Bob Goldstein

Correspondence

smithfw@live.unc.edu

In Brief

Smith et al. show that the body plan of an animal phylum, Tardigrada, originated by loss of a large part of the body. This part corresponds to the entire thorax and nearly the entire abdomen of insects. The results show that the body architecture of a phylum can evolve by a more dramatic loss of body parts than had been anticipated.

Smith et al., 2016, Current Biology *26*, 224–229
January 25, 2016
http://dx.doi.org/10.1016/j.cub.2015.11.059

CellPress

CellPress

Current Biology
Report

The Compact Body Plan of Tardigrades Evolved by the Loss of a Large Body Region

Frank W. Smith,[1,*] Thomas C. Boothby,[1] Ilaria Giovannini,[2] Lorena Rebecchi,[2] Elizabeth L. Jockusch,[3] and Bob Goldstein[1]
[1]Department of Biology, University of North Carolina at Chapel Hill, Chapel Hill, NC 27599, USA
[2]Department of Life Sciences, University of Modena and Reggio Emilia, Modena, via Campi 213/D, 41125 Modena, Italy
[3]Department of Ecology & Evolutionary Biology, University of Connecticut, Storrs, CT 06269, USA
*Correspondence: smithfw@live.unc.edu
http://dx.doi.org/10.1016/j.cub.2015.11.059

SUMMARY

The superphylum Panarthropoda (Arthropoda, Onychophora, and Tardigrada) exhibits a remarkable diversity of segment morphologies, enabling these animals to occupy diverse ecological niches. The molecular identities of these segments are specified by Hox genes and other axis patterning genes during development [1, 2]. Comparisons of molecular segment identities between arthropod and onychophoran species have yielded important insights into the origins and diversification of their body plans [3–9]. However, the relationship of the segments of tardigrades to those of arthropods and onychophorans has remained enigmatic [10, 11], limiting our understanding of early panarthropod body plan diversification. Here, we reveal molecular identities for all of the segments of a tardigrade. Based on our analysis, we conclude that tardigrades have lost a large intermediate region of the body axis—a region corresponding to the entire thorax and most of the abdomen of insects—and that they have lost the Hox genes that originally specified this region. Our data suggest that nearly the entire tardigrade body axis is homologous to just the head region of arthropods. Based on our results, we reconstruct a last common ancestor of Panarthropoda that had a relatively elongate body plan like most arthropods and onychophorans, rather than a compact, tardigrade-like body plan. These results demonstrate that the body plan of an animal phylum can originate by the loss of a large part of the body.

RESULTS AND DISCUSSION

Understanding the origin of animal body plans has been a long-standing issue in evolutionary biology, ever since Darwin struggled to reconcile his theory with the early fossil record of animals [12]. The body plans of the panarthropod phyla are based on a conserved segmental architecture. Within this conserved architecture exists an incredible degree of morphological diversification, to an extent that recognizing homologous segmented regions among distantly related panarthropods has historically been difficult. Recently, this difficulty has been circumvented in onychophoran and arthropod studies by identifying homologous segmented regions based on their molecular identities [3–8]. The body plan of tardigrades is relatively compact and invariant, consisting of just a head and four leg-bearing segments (Figure 1). Understanding panarthropod body plan diversification requires insight into the relationships of tardigrade segments to those of arthropods and onychophorans; indeed, this is important for deciphering the ancestral condition from which all panarthropods diversified. However, nothing is known about molecular identities of tardigrade segments, impeding our understanding of body plan diversification within Panarthropoda.

Hox genes provide molecular identities to regions of the anteroposterior body axis across Bilateria [1]. To illuminate the molecular identities of tardigrade segments, we initially focused our investigation on the Hox genes of the tardigrade *Hypsibius dujardini*. We identified the same set of candidate Hox genes in our *H. dujardini* genome [13] and in mixed-stage transcriptome assemblies. Based on a phylogenetic analysis (Figure S1A) and the presence of diagnostic protein residues (Figure S1C), we identified orthologs of five Hox genes (Figure 2 and Table S1): *labial* (*Hd-lab*), *Hox3* (*Hd-Hox3*), *Deformed* (*Hd-Dfd*), *fushi tarazu* (*Hd-ftz*), and three *Abdominal-B* paralogs (*Hd-Abd-B1–Hd-Abd-B3*). The Hox genes *proboscipedia* (*pb*), *Sex combs reduced* (*Scr*), *Antennapedia* (*Antp*), and at least one representative of *Ultrabithorax* (*Ubx*) and *abdominal-A* (*abd-A*) are reconstructed as ancestral for Panarthropoda [14] but are absent in our *H. dujardini* genome and transcriptome assemblies. To verify that the *H. dujardini* complement of Hox genes is representative of tardigrades, we looked for Hox genes in the transcriptomes of two distantly related tardigrade species, *Paramacrobiotus richtersi* and *Milnesium tardigradum* [16], which, with *H. dujardini*, span the class Eutardigrada [17]. We identified the same set of Hox orthologs in these species as we did in *H. dujardini* (Figures 2, S1B, and S1C and Table S1) but with only single copies of *Abd-B* in *P. richtersi* and *M. tardigradum*.

Our analyses suggest three interesting features concerning the evolution of the tardigrade Hox gene complex. First, an analysis of nucleotide sequences suggests that ancestral tardigrades had a single copy of *Abd-B*, which gave rise to *Hd-Abd-B1–Hd-Abd-B3* through duplication events in the *H. dujardini* lineage (Figure S1B′). Supporting this conclusion, the predicted Abd-B protein sequences of *H. dujardini* share unique residues at two positions within the homeodomain where the other tardigrades of this study exhibit residues characteristic of other panarthropods (Figure S1C). In terms of protein

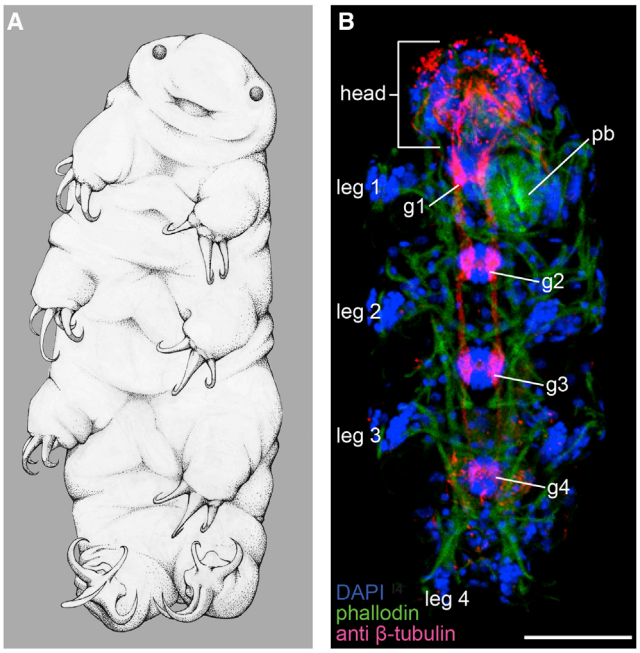

Figure 1. The Tardigrade Body Plan

(A) Illustration of a *H. dujardini* specimen, based on a scanning electron micrograph (body) and transmitted light micrographs (eyes) by Anya Broverman-Wray, used with permission.

(B) *H. dujardini* specimen with DAPI-stained nuclei, phalloidin-stained muscles, and nervous system visualized using a β-tubulin antibody. g1–g4, ganglion 1 through ganglion 4; pb, pharyngeal bulb. The scale bar represents 20 μm.

sequence similarity, compared to *Hd*-Abd-B2 (Figure S1A), or in terms of the length of the predicted protein sequence, compared to *Hd*-Abd-B3 (Figure S2B), the predicted protein sequence of *Hd-Abd-B1* most closely resembles Abd-B sequences from other panarthropods, so we narrowed our focus to this paralog. Second, our analyses suggest that *pb*, *Scr*, *Antp*, and *Ubx/abd-A* orthologs were lost in the tardigrade lineage (Figure 2), an unprecedented degree of loss in Panarthropoda. Third, unlike in many animal genomes [14, 15], in the *H. dujardini* genome, several predicted protein-coding genes are dispersed among Hox genes (Figures 2 and S3). This result is consistent with the loss of some Hox genes and disorganization of the Hox cluster seen together in certain other animal genomes [18]. Tardigrade segments develop simultaneously [19, 20]; disorganization of the Hox cluster has been suggested to be a prerequisite for the evolution of this developmental mode [21].

Next, we developed in situ hybridization methods for tardigrades, and we used these methods to determine the embryonic expression domains of *H. dujardini* Hox genes. We found an anterior-to-posterior order of expression domains that is similar to the order seen in other animals. At 35 hr post egg laying (hpl), *Hd-lab* exhibited the strongest expression in the first leg-bearing segment; by 55 hpl, strong expression of this gene was confined to the pharyngeal bulb (Figures 3B, 3I, and S4A). We detected strongest expression of *Hd-Hox3* in the second and third leg-bearing segments, which resolved into expression in the ganglion of the second leg-bearing segment and the legs of the second and third leg-bearing segments by 55 hpl (Figures 3C, 3I, and S4B). Throughout development, *Hd-Dfd* exhibited localized expression near the developing ganglion of the third leg-bearing segment (Figures 3D, 3I, and S4C). *Hd-ftz* signal developed in an anterior region of the fourth leg-bearing segment, with strong expression near the ganglion of this segment at 55 hpl (Figures 3E, 3I, and S4D). Finally, *Hd-Abd-B1* expression was strongest in a posterior region of the fourth leg-bearing segment, which included the base of the legs (Figures 3F, 3I, and S4E).

Previously, researchers have compared anterior expression boundaries of Hox genes to identify homologous segments across the Onychophora and Arthropoda [3–6]. The anterior expression domains of *Hd-Hox3*, *Hd-Dfd*, and *Hd-ftz* match the expression domains of their homologs in arthropods and onychophorans if tardigrade segments are aligned one to one with onychophoran and arthropod segments in anteroposterior order (Figure 4A). This alignment suggests that the tardigrade body axis is primarily homologous to just the head region of arthropods and directly supports the hypothesis that the diversity of head appendages of arthropods and onychophorans evolved from legs [6, 24, 25]. This result also addresses a current debate about whether the tardigrade head is homologous to several anterior segments of arthropods [26, 27], or whether it is composed of a single segment [28]. Our alignment of segments based on Hox gene expression supports the latter hypothesis (Figure 4A). To further test the composition of the tardigrade head, we investigated embryonic expression of the head gap gene *orthodenticle* (*otd*), which is restricted to the first segment in most arthropods and onychophorans during early stages of segmentation [4, 22, 23]. *Hd-otd* exhibited strong expression broadly across the head of *H. dujardini* during early stages of segmentation (Figure 3G), buttressing our conclusion that the head of tardigrades is homologous to the first segment of other panarthropods. While we generally found conservation of gene expression patterns, *Hd-lab* was expressed at relatively high levels in the second segment (Figures 3B and 3I), unlike in other panarthropods [3–9]. Under our model of segment homologies (Figure 4A), this implies that there has been an anterior expansion of *lab* expression in the tardigrade lineage or a posterior retraction of *lab* expression in other panarthropods. We cannot confidently discriminate between these possibilities.

Our model of segment homologies suggests that the tardigrade body axis is reduced, relative to other panarthropods, comprising mostly anterior identity, in line with an earlier hypothesis based on nervous system anatomy [29]. How did this evolve? The expression pattern of the posterior marker *Hd-Abd-B1* suggests that posterior identity is retained in the posterior of the tardigrade body axis, which indicates that simple truncation is not the answer. Expression of the posterior marker *caudal* (*cad*) [30, 31] in a posterior region of the fourth leg-bearing segment (Figures 3H and 3I) confirms the retention of posterior identity. In other panarthropods [8] and distantly related annelid worms [14], an extensive intermediate trunk region is defined by expression of orthologs of *Antp*, *Ubx*, and *abd-A*, genes that have been lost in the tardigrade lineage (Figure 4B). In *H. dujardini*, the anterior borders of *ftz* and *Abd-B* expression lie in the same segment, precluding the existence of segments with intermediate Hox identities between these markers in this species. Therefore, we propose that the reduced body axis of

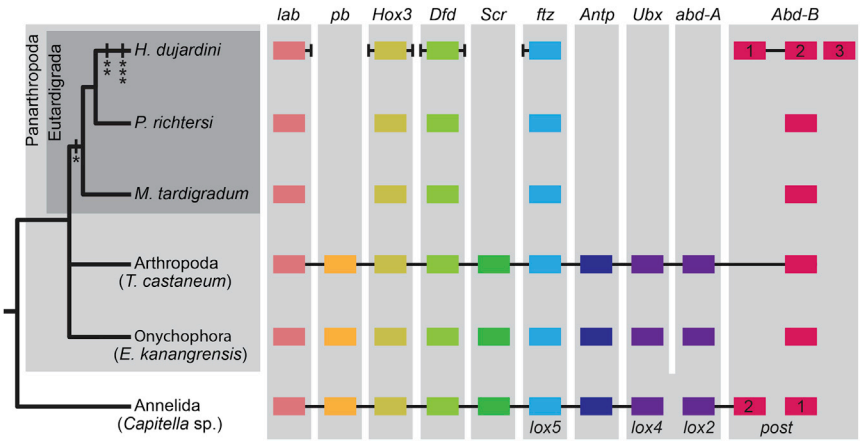

Figure 2. Hox Cluster Evolution in Tardigrada

Asterisks (*, **, and ***) indicate the following: loss of *pb*, *Scr*, *Antp*, and *Ubx/abd-A* ortholog(s), most likely in several events (*); first duplication of *Abd-B*, giving rise to *Abd-B2* and the common ancestor of *Abd-B1* and *Abd-B3* (**); duplication event giving rise to *Abd-B1* and *Abd-B3* (***). Unique annelid Hox gene ortholog names are provided below the colored Hox symbols. Horizontal black lines connect Hox genes in cases where open reading frames (ORFs) are not found between these Hox genes in the genome. Vertical black lines represent cases where ORFs are predicted to separate Hox genes in the genome. Black lines are not shown for cases where genomic data are not available to distinguish between these possibilities. Non-tardigrade Hox gene information based on [8, 14, 15]. See also Figures S1, S2, and S3 and Table S1.

tardigrades evolved through the loss of an intermediate trunk region in this lineage, a region corresponding to the entire thorax and most of the abdomen in insects. Based on our evidence supporting a reduction of the body axis in the tardigrade lineage, we conclude that a compact body plan is a tardigrade novelty, while the panarthropod ancestor possessed a more elongate body plan (Figure 4C). This conclusion is insensitive to the interrelationships of the panarthropod lineages; whether Tardigrada is the sister group of Arthropoda [32] or the earliest diverging panarthropod phylum [33, 34] is currently under debate.

The loss of Hox genes is unlikely to be the cause of segment loss because Hox genes typically specify segment identities rather than regulate segment production [35]. Supporting this idea, the loss of *pb* and *Scr* in the tardigrade lineage does not appear to correspond to the loss of any particular segment. However, Hox genes might become dispensable when the segments they once specified are lost, leading to loss of such Hox genes through neutral processes [35]. We suggest that the loss of *Antp* and *Ubx/abd-A* in the genomes of tardigrades followed the loss of the intermediate segments they originally specified. Unlike in tardigrades [19, 20], in many panarthropods and other animals a large fraction of the body axis develops by terminal addition through posterior growth; terminal addition may be ancestral for Bilateria [36] and has been suggested to be a trait of a stem group tardigrade lineage [37]. We speculate that reduction, and ultimately loss, of terminal addition accounts for the loss of intermediate segments in the tardigrade lineage. In this view, most of the tardigrade body axis represents the short germband of other panarthropods, i.e., the few anterior segments that appear simultaneously during development

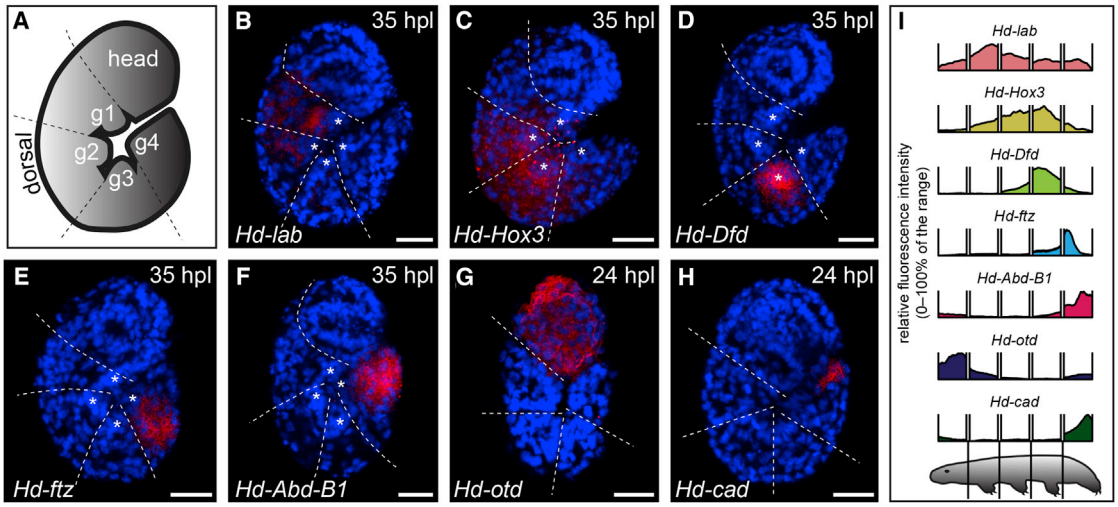

Figure 3. Expression Patterns of *H. dujardini* Homeobox Genes

(A) Diagram of a 35 hpl embryo. g1–g4, ganglion 1 through ganglion 4.

(B–H) Maximum projection of fluorescent in situ hybridizations. Gene expression is shown in red. DAPI, which stains nuclei, is shown in blue. Dashed lines represent segment boundaries; boundaries are inferred by DAPI staining and body morphology. Asterisks denote positions of ganglia. Scale bars represent 10 μm.

(I) Quantifications of fluorescent in situ intensities in (B)–(H). Trend lines are 50 0.08-μm moving averages, calculated for each segment separately, from 0% to 100% segment length for each segment. For each gene, fluorescence intensity is scaled to the range of intensities detected (0%–100% of the range).

See also Figure S4.

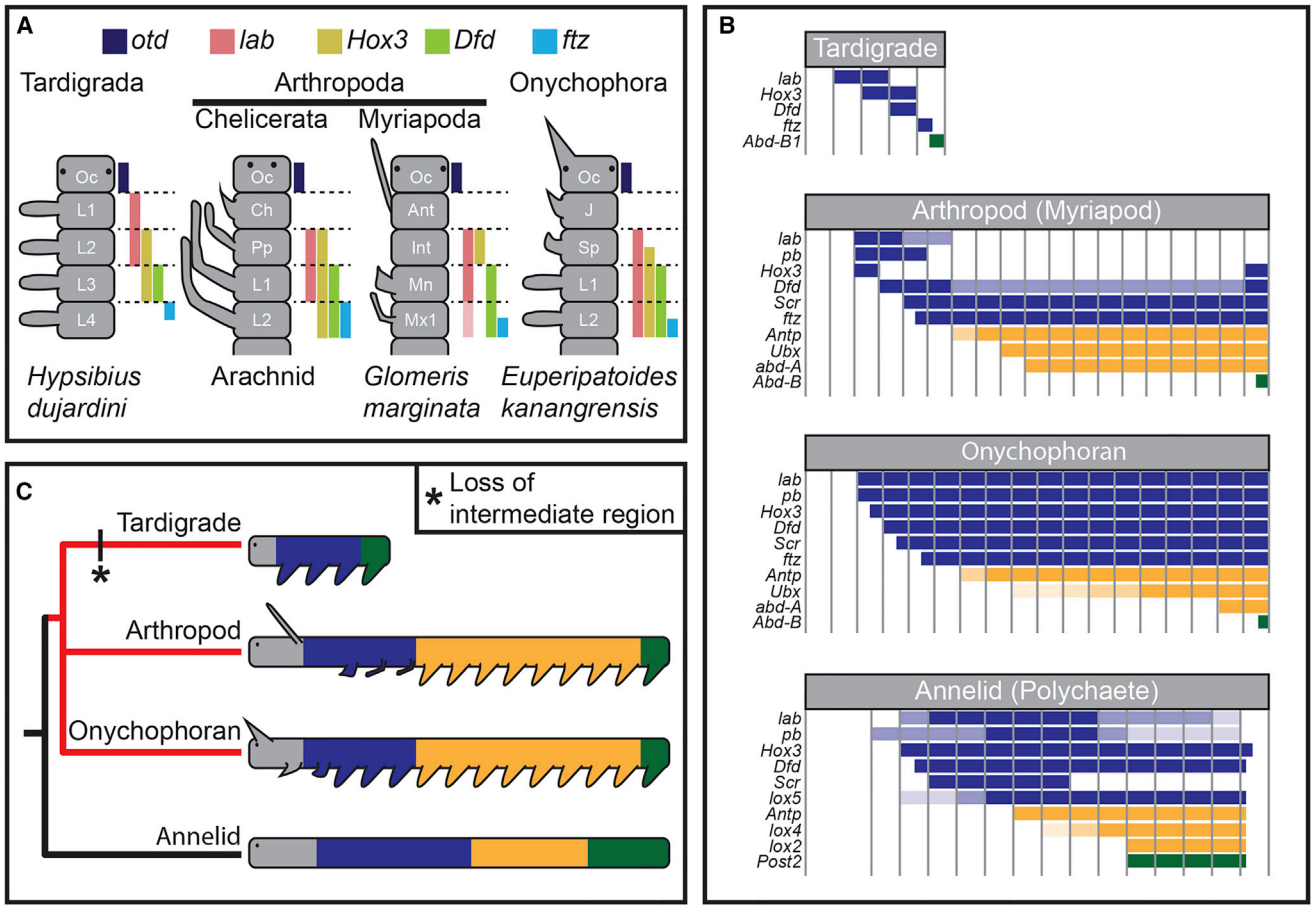

Figure 4. The Evolution of the Tardigrade Body Plan

(A) Hypothesized alignment of tardigrade segments with anterior segments of other panarthropods. Data from other panarthropods based on [4, 7–9, 22, 23]. Ant, antenna; Ch, chelicera; Int, intercalary; J, jaw; L1–L4, legs; Mn, mandible; Mx1, maxilla 1; Oc, ocular; Pp, pedipalp; Sp, slime papilla.

(B) Comparison of Hox gene expression domains. Hox gene expression domains are colored based on location of segments they specify in many panarthropod species: blue, anterior; orange, intermediate; green, posterior. Tardigrade, *H. dujardini*; Arthropod, *Glomeris marginata* [9]; Onychophoran, *Euperipatoides kanangrensis* [8]; Annelid, *Capitella* sp. [14]. See [2] for Hox gene expression patterns in additional arthropod species.

(A and B) Darker shading represents higher expression or broader expression.

(C) Hypothesis for the evolution of the tardigrade body plan by the loss of an intermediate trunk region (orange). Panarthropod branches are red in the phylogenetic tree.

before terminal segment addition commences. This model would require that the posterior region of the short germband be respecified as the posterior of the body axis, since segments with posterior-most identity are normally the last segments to emerge through terminal addition, and posterior identity is retained in tardigrades. Diversity in segment number in other panarthropods emerges in the body region that is produced through terminal addition. We speculate that the loss of terminal addition in the tardigrade lineage explains the invariant segment number of this phylum.

EXPERIMENTAL PROCEDURES

Assembly and Annotation

Transcriptome assemblies were derived from 100 bp paired-end Illumina reads or from reads downloaded from NCBI's SRA database (accessions SRX426237–SRX426240) and assembled using Trinity [38] (T.C.B., unpublished data). Our genome assembly was derived from short insert mate pair and Moleculo long read libraries generated from DNA extracted from *H. dujardini* [13]. Assembly was performed with the Celera assembler version 8.1 [39]. Annotations for the *H. dujardini* genome assembly were generated using the automated genome annotation pipeline MAKER2 [40]. Our *H. dujardini* genome sequencing resulted in an assembly of 212.3 Mb with an average estimated coverage of 126X. Our assembly contains 95.16% of core eukaryotic genes (CEGMA).

Gene Identification

We identified candidate genes in our genome and transcriptome databases by reciprocal BLAST searches using arthropod and onychophoran sequences as queries. For phylogenetic analyses, we used alignments of homeodomain protein sequences or homeobox nucleotide sequences. Our amino acid matrix was based on the matrix used to identify Hox orthologs in an onychophoran [8]. We implemented the LG model [41] (for amino acid alignments) or the HKY85 model [42] (for nucleotide alignments) with an estimated gamma shape parameter with four substitution rate categories. Maximum likelihood analyses were performed with PhyML [43] with 500 bootstrap replicates. Bayesian analyses were performed in MrBayes [44]. Amino acid analyses ran for 1,200,000

generations. The nucleotide analysis ran for 600,000 generations. Posterior tree distributions were sampled every 100 generations. Burn-in = 7,500 for amino acid analyses; burn-in = 1,500 for nucleotide analysis.

Cloning

We amplified genes from embryonic *H. dujardini* cDNA by PCR and cloned PCR products into the pCR4-TOPO vector (Invitrogen). Primers used in this study were as follows: *Hd-lab*, 5′-CAGGATGCTCGCTATGCTAATTCCA-3′, 5′-AGTCTCATTGAGGGAGAGCTGGTT-3′; *Hd-Hox3*, 5′-GGAGCAGCAGACCTTTTCTCCTAC-3′, 5′-CGCAATCACTTTTAGGGATGGACCT-3′; *Hd-Dfd*, 5′-CATTTGGCTCCATGCCTTATCAGTC-3′, 5′-TGGTGTTGGGCAATTTATGGTCCT-3′; *Hd-ftz*, 5′-GTACCACTACTGCACGTCCTTACAG-3′, 5′-TCTCCAGCTTCTTCTCCTTCTTGTAC-3′; *Hd-Abd-B1*, 5′-ATCGACAACTTCCCGTCCTATCAC-3′, 5′-GTTGGTGGAACTTTTGTGGTTGGA-3′; *Hd-otd*, 5′-GTTCCCGCACCGAGGAAACAG-3′, 5′-CTCTCACGTCCTCCACGCTGA-3′; *Hd-cad*, 5′-ATCATCCGGCGTACAATATGAACA-3′, 5′-AAATGGGCGACTCTCATAAACAGC-3′.

In Situ Hybridization

Digoxigenin-labeled probes were produced using T3 or T7 RNA polymerase (Promega). Sense strand probes were used as negative controls. Embryos were removed from parental exuviae with a 25G needle and then permeabilized in a 5 U/ml chitinase (Sigma), 10 mg/ml chymotrypsin (Sigma) solution in 50 mM potassium phosphate buffer (pH 6.0) for 1 hr. Embryos were rinsed three times for 5 min in 0.5X PBtween (0.5X PBS; 0.1% Tween20; in DEPC water) and fixed in a 4% paraformaldehyde, 33% heptane solution in 0.5X PBtween for 30 min while shaking vigorously. This was followed by five washes for 5 min each in 0.5X PBtween. Embryos were then rinsed in 25%, 50%, 70%, and 90% methanol in 0.5X PBtween for 5 min each, followed by three washes in 100% methanol, and stored at −20°C. Before hybridization, embryos were taken through a reverse graded series of methanol washes, followed by three washes in 0.5X PBtween. Embryos were removed from their eggshells with a 25G needle. The acetylation and hybridization steps followed existing procedures designed to minimize loss of small embryos [45], with 0.5X PBtween substituted for 1X PBtween, and 20X SSC at pH 6.0 substituted for 20X SSC at pH 4.5. We added 1 μl of boiled and sheared salmon sperm (40 mg/ml) to probe solution (final concentration ~0.5 μg/ml DIG-labeled riboprobe in Hybe buffer [50% formamide; 25% 20X SSC, pH 6.0; 0.1% Tween20; in DEPC water]) after the probe was heated rather than adding salmon sperm directly to the Hybe buffer. We hybridized probes for 16 hr at 60°C. Post-hybridization washes were performed at 60°C with all buffers heated to this temperature. Embryos were washed five times quickly, followed by five 20-min washes in plain Hybe buffer. Next we washed embryos five times quickly and for 30 min with 2X SSC, 0.1% CHAPS. This was followed by two 30-min washes with 1X SSC, 0.1% CHAPS and two 30-min washes with 0.2X SSC, 0.1% CHAPS. We then washed embryos twice with 0.5X PBtween at room temperature. Embryos were incubated in blocking solution (2% BSA; 50% blocking reagent solution [BRS]; in 0.5X PBtween) for 2 hr at room temperature. BRS consists of 10% blocking reagent (Roche) in maleic acid buffer (pH 7.5). Embryos were incubated overnight at 4°C in 1:1,500 anti-DIG-AP (Roche) in blocking solution. Next, embryos were washed five times quickly and five times for 10 min in maleic acid buffer (pH 7.5). We then washed embryos three times quickly in alkaline phosphatase developing solution (100 mM NaCl; 50 mM MgCL; 100 mM Tris, pH 9.5; 0.1% Tween20). We developed in situ signal in BM Purple (Roche). To stop development of the in situ reaction, we washed embryos in 0.5X PBtween. Embryos were then post-fixed in 100% ethanol for 3 min, followed by a 0.5X PBtween wash.

Imaging and Quantification

Embryos were mounted in DAPI Fluoromount-G (SouthernBiotech). To collect fluorescent in situ data, we took advantage of the fluorescent properties of the chromogenic precipitate [46]. z stacks were captured on a Zeiss 710 LSM using an EC Plan-Neofluor 100×/1.30 oil objective, 633 nm excitation wavelength, with data collected for emission wavelengths between 685 and 759 nm. Maximum projections were produced in ImageJ. Maximum projections are from slices of a z stack of the medial region of embryos in all cases except Figure 3G, which shows the lateral region of the embryo. In ImageJ, a ten-pixel-wide line scan of the ventral embryonic region of maximum projections was used to measure fluorescent intensity. The fluorescence intensities we report are from raw data. We adjusted the brightness and contrast of images for figures in ImageJ. Methods used for phalloidin staining and anti β-tubulin staining were previously published [10].

ACCESSION NUMBERS

See Table S1 for a full list of GenBank accession numbers for genes reported in this study.

SUPPLEMENTAL INFORMATION

Supplemental Information includes four figures and one table and can be found with this article online at http://dx.doi.org/10.1016/j.cub.2015.11.059.

AUTHOR CONTRIBUTIONS

F.W.S. and B.G. designed this study. F.W.S. developed the in situ protocol in consultation with E.L.J. and B.G. F.W.S. collected and analyzed data and wrote the first draft of the manuscript. T.C.B. performed genome and transcriptome analyses. I.G. and L.R. provided transcriptomic data for *P. richtersi*. All authors read, made contributions to, and approved this manuscript.

ACKNOWLEDGMENTS

This work was funded by NSF grant no. IOS-1257320 to B.G. and an EDEN award (NSF/EDEN grant no. IOS-0955517) to F.W.S. I.G. and L.R. were funded by Azioni di mobilità internazionale per collaborazione scientifica e culturale tra l'Università di Modena e Reggio Emilia e Università straniere. B.G. lab members Timothy Cupp, Daniel Dickinson, Jennifer Heppert, Ariel Pani, and Sophia Tintori provided helpful discussion of this work. We are indebted to David Angelini, Austen Barnett, Cassandra Extavour, Christopher Owen, Prashant Sharma, Chris Lowe, and Greg Wray for helpful comments on this manuscript. We thank all four anonymous reviewers for helpful comments that improved the quality of our manuscript.

Received: October 8, 2015
Revised: November 12, 2015
Accepted: November 12, 2015
Published: January 14, 2016

REFERENCES

1. McGinnis, W., and Krumlauf, R. (1992). Homeobox genes and axial patterning. Cell *68*, 283–302.
2. Hughes, C.L., and Kaufman, T.C. (2002). Hox genes and the evolution of the arthropod body plan. Evol. Dev. *4*, 459–499.
3. Damen, W.G., Hausdorf, M., Seyfarth, E.A., and Tautz, D. (1998). A conserved mode of head segmentation in arthropods revealed by the expression pattern of Hox genes in a spider. Proc. Natl. Acad. Sci. USA *95*, 10665–10670.
4. Telford, M.J., and Thomas, R.H. (1998). Expression of homeobox genes shows chelicerate arthropods retain their deutocerebral segment. Proc. Natl. Acad. Sci. USA *95*, 10671–10675.
5. Jager, M., Murienne, J., Clabaut, C., Deutsch, J., Le Guyader, H., and Manuel, M. (2006). Homology of arthropod anterior appendages revealed by Hox gene expression in a sea spider. Nature *441*, 506–508.
6. Eriksson, B.J., Tait, N.N., Budd, G.E., Janssen, R., and Akam, M. (2010). Head patterning and Hox gene expression in an onychophoran and its implications for the arthropod head problem. Dev. Genes Evol. *220*, 117–122.
7. Sharma, P.P., Schwager, E.E., Extavour, C.G., and Giribet, G. (2012). Hox gene expression in the harvestman *Phalangium opilio* reveals divergent patterning of the chelicerate opisthosoma. Evol. Dev. *14*, 450–463.

8. Janssen, R., Eriksson, B.J., Tait, N.N., and Budd, G.E. (2014). Onychophoran Hox genes and the evolution of arthropod Hox gene expression. Front. Zool. *11*, 22.
9. Janssen, R., and Damen, W.G. (2006). The ten Hox genes of the millipede *Glomeris marginata*. Dev. Genes Evol. *216*, 451–465.
10. Smith, F.W., and Jockusch, E.L. (2014). The metameric pattern of *Hypsibius dujardini* (Eutardigrada) and its relationship to that of other panarthropods. Front. Zool. *11*, 66.
11. Marchioro, T., Rebecchi, L., Cesari, M., Hansen, J.G., Viotti, G., and Guidetti, R. (2013). Somatic musculature of Tardigrada: phylogenetic signal and metameric patterns. Zool. J. Linn. Soc. *169*, 580–603.
12. Darwin, C. (1859). On the sudden appearance of whole groups of Allied Species. In On the Origin of Species (John Murray), pp. 306–311.
13. Boothby, T.C., Tenlen, J.R., Smith, F.W., Wang, J.R., Patanella, K.A., Osborne Nishimura, E., Tintori, S.C., Li, Q., Jones, C.D., Yandell, M., et al. (2015). Evidence for extensive horizontal gene transfer from the draft genome of a tardigrade. Proc. Natl. Acad. Sci. USA *112*, 15976–15981.
14. Fröbius, A.C., Matus, D.Q., and Seaver, E.C. (2008). Genomic organization and expression demonstrate spatial and temporal Hox gene colinearity in the lophotrochozoan *Capitella* sp. I. PLoS ONE *3*, e4004.
15. Shippy, T.D., Ronshaugen, M., Cande, J., He, J., Beeman, R.W., Levine, M., Brown, S.J., and Denell, R.E. (2008). Analysis of the *Tribolium* homeotic complex: insights into mechanisms constraining insect Hox clusters. Dev. Genes Evol. *218*, 127–139.
16. Wang, C., Grohme, M.A., Mali, B., Schill, R.O., and Frohme, M. (2014). Towards decrypting cryptobiosis—analyzing anhydrobiosis in the tardigrade *Milnesium tardigradum* using transcriptome sequencing. PLoS ONE *9*, e92663.
17. Bertolani, R., Guidetti, R., Marchioro, T., Altiero, T., Rebecchi, L., and Cesari, M. (2014). Phylogeny of Eutardigrada: new molecular data and their morphological support lead to the identification of new evolutionary lineages. Mol. Phylogenet. Evol. *76*, 110–126.
18. Seo, H.C., Edvardsen, R.B., Maeland, A.D., Bjordal, M., Jensen, M.F., Hansen, A., Flaat, M., Weissenbach, J., Lehrach, H., Wincker, P., et al. (2004). Hox cluster disintegration with persistent anteroposterior order of expression in *Oikopleura dioica*. Nature *431*, 67–71.
19. Gabriel, W.N., McNuff, R., Patel, S.K., Gregory, T.R., Jeck, W.R., Jones, C.D., and Goldstein, B. (2007). The tardigrade *Hypsibius dujardini*, a new model for studying the evolution of development. Dev. Biol. *312*, 545–559.
20. Hejnol, A., and Schnabel, R. (2005). The eutardigrade *Thulinia stephaniae* has an indeterminate development and the potential to regulate early blastomere ablations. Development *132*, 1349–1361.
21. Duboule, D. (2007). The rise and fall of Hox gene clusters. Development *134*, 2549–2560.
22. Eriksson, B.J., Samadi, L., and Schmid, A. (2013). The expression pattern of the genes *engrailed, pax6, otd* and *six3* with special respect to head and eye development in *Euperipatoides kanangrensis* Reid 1996 (Onychophora: Peripatopsidae). Dev. Genes Evol. *223*, 237–246.
23. Janssen, R., Budd, G.E., and Damen, W.G. (2011). Gene expression suggests conserved mechanisms patterning the heads of insects and myriapods. Dev. Biol. *357*, 64–72.
24. Angelini, D.R., Smith, F.W., and Jockusch, E.L. (2012). Extent with modification: Leg patterning in the beetle *Tribolium castaneum* and the evolution of serial homologs. G3 (Bethesda) *2*, 235–248.
25. Ma, X., Hou, X., and Bergström, J. (2009). Morphology of *Luolishania longicruris* (Lower Cambrian, Chengjiang Lagerstätte, SW China) and the phylogenetic relationships within lobopodians. Arthropod Struct. Dev. *38*, 271–291.
26. Persson, D.K., Halberg, K.A., Jørgensen, A., Møbjerg, N., and Kristensen, R.M. (2012). Neuroanatomy of *Halobiotus crispae* (Eutardigrada: Hypsibiidae): tardigrade brain structure supports the clade Panarthropoda. J. Morphol. *273*, 1227–1245.
27. Persson, D.K., Halberg, K.A., Jørgensen, A., Møbjerg, N., and Kristensen, R.M. (2014). Brain anatomy of the marine tardigrade *Actinarctus doryphorus* (Arthrotardigrada). J. Morphol. *275*, 173–190.
28. Mayer, G., Kauschke, S., Rüdiger, J., and Stevenson, P.A. (2013). Neural markers reveal a one-segmented head in tardigrades (water bears). PLoS ONE *8*, e59090.
29. Dewel, R.A., and Dewel, W.C. (1996). The brain of *Echiniscus viridissimus* Peterfi, 1956 (Heterotardigrada): a key to understanding the phylogenetic position of tardigrades and the evolution of the arthropod head. Zool. J. Linn. Soc. *116*, 35–49.
30. Shinmyo, Y., Mito, T., Matsushita, T., Sarashina, I., Miyawaki, K., Ohuchi, H., and Noji, S. (2005). *caudal* is required for gnathal and thoracic patterning and for posterior elongation in the intermediate-germband cricket *Gryllus bimaculatus*. Mech. Dev. *122*, 231–239.
31. Wu, L.H., and Lengyel, J.A. (1998). Role of *caudal* in hindgut specification and gastrulation suggests homology between *Drosophila* amnioproctodeal invagination and vertebrate blastopore. Development *125*, 2433–2442.
32. Smith, M.R., and Ortega-Hernández, J. (2014). *Hallucigenia*'s onychophoran-like claws and the case for Tactopoda. Nature *514*, 363–366.
33. Campbell, L.I., Rota-Stabelli, O., Edgecombe, G.D., Marchioro, T., Longhorn, S.J., Telford, M.J., Philippe, H., Rebecchi, L., Peterson, K.J., and Pisani, D. (2011). MicroRNAs and phylogenomics resolve the relationships of Tardigrada and suggest that velvet worms are the sister group of Arthropoda. Proc. Natl. Acad. Sci. USA *108*, 15920–15924.
34. Legg, D.A., Sutton, M.D., and Edgecombe, G.D. (2013). Arthropod fossil data increase congruence of morphological and molecular phylogenies. Nat. Commun. *4*, 2485.
35. Barnett, A.A., and Thomas, R.H. (2013). Posterior Hox gene reduction in an arthropod: *Ultrabithorax* and *Abdominal-B* are expressed in a single segment in the mite *Archegozetes longisetosus*. Evodevo *4*, 23.
36. Gold, D.A., Runnegar, B., Gehling, J.G., and Jacobs, D.K. (2015). Ancestral state reconstruction of ontogeny supports a bilaterian affinity for *Dickinsonia*. Evol. Dev. *17*, 315–324.
37. Maas, A., and Waloszek, D. (2001). Cambrian derivatives of the early arthropod stem lineage, pentastomids, tardigrades and lobopodians – an 'Orsten' perspective. Zool. Anz. *240*, 451–459.
38. Haas, B.J., Papanicolaou, A., Yassour, M., Grabherr, M., Blood, P.D., Bowden, J., Couger, M.B., Eccles, D., Li, B., Lieber, M., et al. (2013). De novo transcript sequence reconstruction from RNA-seq using the Trinity platform for reference generation and analysis. Nat. Protoc. *8*, 1494–1512.
39. Myers, E.W., Sutton, G.G., Delcher, A.L., Dew, I.M., Fasulo, D.P., Flanigan, M.J., Kravitz, S.A., Mobarry, C.M., Reinert, K.H., Remington, K.A., et al. (2000). A whole-genome assembly of *Drosophila*. Science *287*, 2196–2204.
40. Holt, C., and Yandell, M. (2011). MAKER2: an annotation pipeline and genome-database management tool for second-generation genome projects. BMC Bioinformatics *12*, 491.
41. Le, S.Q., and Gascuel, O. (2008). An improved general amino acid replacement matrix. Mol. Biol. Evol. *25*, 1307–1320.
42. Hasegawa, M., Kishino, H., and Yano, T. (1985). Dating of the human-ape splitting by a molecular clock of mitochondrial DNA. J. Mol. Evol. *22*, 160–174.
43. Guindon, S., Dufayard, J.F., Lefort, V., Anisimova, M., Hordijk, W., and Gascuel, O. (2010). New algorithms and methods to estimate maximum-likelihood phylogenies: assessing the performance of PhyML 3.0. Syst. Biol. *59*, 307–321.
44. Huelsenbeck, J.P., and Ronquist, F. (2005). Bayesian analysis of molecular evolution using MrBayes. In Statistical Methods in Molecular Evolution, R. Nielsen, ed. (Springer), pp. 183–226.
45. Irvine, S.Q. (2007). Whole-mount *in situ* hybridization of small invertebrate embryos using laboratory mini-columns. Biotechniques *43*, 764–768, 766, 768.
46. Trinh, A., McCutchen, M.D., Bonner-Fraser, M., Fraser, S.E., Bumm, L.A., and McCauley, D.W. (2007). Fluorescent *in situ* hybridization employing the conventional NBT/BCIP chromogenic stain. Biotechniques *42*, 756–759.